

Chapter 4

Numerical Results

Abstract We develop a computational scheme for the parabolic renormalization operator which is based on the asymptotics of the Fatou coordinates at infinity, and apply it to numerical computations of the basin and the domain of the renormalization fixed point and of the spectrum of the parabolic renormalization operator at the fixed point.

Keywords Spectrum of the renormalization operator · Universality

4.1 A Computational Scheme for \mathcal{P}

Having mentioned the resurgent properties of the asymptotic expansion of the Fatou coordinate, we proceed to describe the computational scheme for \mathcal{P} (see Fig. 4.1). We begin with a germ of an analytic mapping

$$f(z) = z + z^2 + O(z^3)$$

defined in a neighborhood of the origin. Applying the change of coordinates $w = \kappa(z) = -1/z$, we obtain

$$F(w) = w + 1 + \frac{A}{w} + O\left(\frac{1}{w^2}\right)$$

defined in a neighborhood of ∞ . We again use the notation $\Phi_A(w)$ for the function that conjugates F with the unit translation

$$\Phi_A(F(w)) = \Phi_A(w) + 1$$

for $\operatorname{Re} w \gg 1$. We let $\Phi_R(w)$ be the solution of the same functional equation for $\operatorname{Re} w \ll -1$. These changes of coordinate are well-defined up to an additive constant, and

$$\phi_A(z) = \kappa^{-1} \circ \Phi_A \circ \kappa(z), \quad \phi_R(z) = \kappa^{-1} \circ \Phi_R \circ \kappa(z).$$

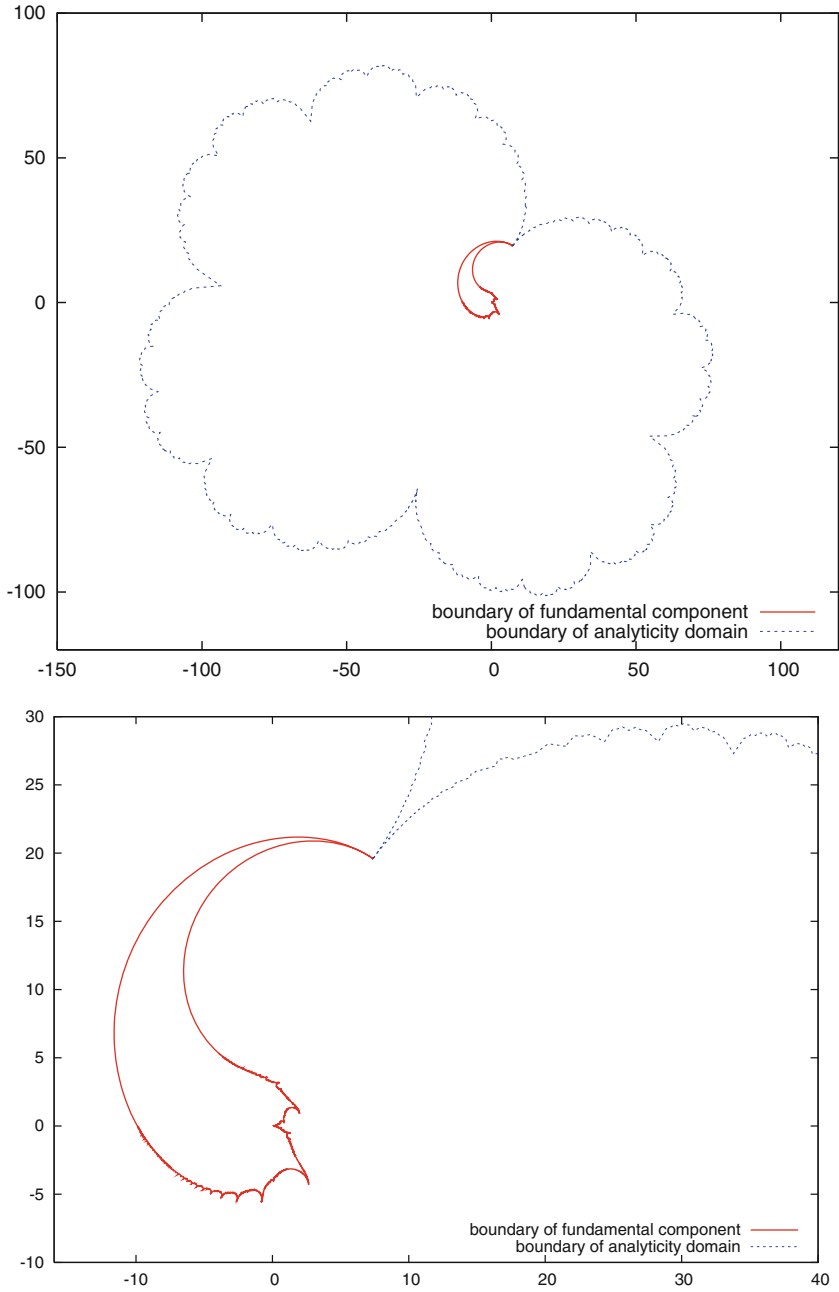


Fig. 4.1 The domain of analyticity of $\mathcal{P} f_0(z)$ for $f_0(z) = z + z^2$, with the immediate parabolic basin indicated

As we have seen in Theorem 2.2, the function $\Phi_A(w)$ has an asymptotic development

$$\Phi_A(w) \sim w - A \log w + \text{const}_A + \sum_{k=1}^{\infty} b_k w^{-k}.$$

The coordinate $\Phi_R(w)$ has an *identical* asymptotic development, differing only by the value of const_R . While this may seem surprising at first glance, recall that these functions are Laplace transforms of *different* analytic continuations of the Borel transform of the same divergent series (plus the $w - A \log w + \text{const}$ term).

We select a large integer M (in practice, $M \approx 100$). We will use the asymptotic expansion to estimate $\Phi_A(w)$ for $w \geq M$ and $\Phi_R(w)$ for $w \leq -M$. Consider an iterate $N \approx 2M$ such that

$$\text{Re } F^N(w) \geq M \quad \text{for } \text{Re } w \in [-M - 1, -M].$$

Let $v(z)$ be the function

$$v(z) = \text{ixp} \circ \Phi_A \circ F^N \circ (\Phi_R)^{-1} \circ \text{ixp}^{-1}(z).$$

It differs from the parabolic renormalization $\mathcal{P}(f)$ only by rescaling the function and its argument:

$$\mathcal{P}(f)(z) = a_1 v(a_0 z).$$

Now consider a contour Γ connecting $w = -M - 1 + iH$ with $F(w) \approx -M + iH$ which is mapped onto the circle $S_\rho = \{|z| = \rho\}$ for a small value of ρ by $\text{ixp} \circ \Phi_R$. Select $n \in \mathbb{N}$ and consider the n points in S_ρ given by $x_k = \rho \exp(2\pi k/n)$, $k = 0, \dots, n - 1$. We then evaluate the first n coefficients in the Taylor expansion of η at the origin

$$\eta(z) = \sum_{j=0}^{\infty} r_j z^j$$

using a discrete Fourier transform. Specifically, we calculate

$$s_k = v(x_k) \approx \sum_{j=0}^{n-1} r_j (x_k)^j = \sum_{j=0}^{n-1} r_j \rho^j \exp(2\pi k j/n),$$

and apply the inverse discrete Fourier transform:

$$r_j \approx \frac{1}{n\rho^j} \sum_{k=0}^{n-1} s_k \exp(-2\pi k j/n).$$

Since

$$\mathcal{P}(f)(z) = \sum_{j=1}^{\infty} s_j a_1 a_0^j z^j,$$

we have

$$a_1 a_0 s_1 = 1, \text{ and further } a_0 = \frac{s_1}{s_2}.$$

This step completes the computation of the Taylor expansion of $\mathcal{P}(f)$.

4.1.1 Computing f_*

In computing the fixed point $f_*(z)$ we find it more convenient to work with the representation of a germ $f(z) = z + z^2 + \dots$ in the form

$$f(z) = z \exp(f_{\log}(z)),$$

where f_{\log} is a germ of an analytic function at the origin with $f_{\log}(z) = z + \dots$. We then rewrite the parabolic renormalization operator in terms of its action on f_{\log} :

$$\mathcal{P}_{\log}(f_{\log})(z) = (2\pi i)^{-1} \Phi_A \circ F^N \circ (\Phi_R)^{-1} \circ \text{ixp}^{-1}(z) - \text{ixp}^{-1}(z).$$

This helps to avoid the round-off error which arises from the growth of f_* near the boundary $\partial \text{Dom}(f_*)$.

Modifying the scheme described above for the operator \mathcal{P}_{\log} , we calculate the fixed point by iterating \mathcal{P} starting at $f_0(z) = z + z^2$:

Empirical Observation 4.1

$$f_*(z) \approx z + z^2 + 0.(514 - 0.0346i)z^3 + \dots$$

Our calculations appear reliable up to the size of the round-off error in double-precision arithmetic ($\sim 10^{-14}$) in the disk of radius $r = 5$ around the origin. As we will see below, the true radius of convergence for the series for f_* is approximately 41 (see the Empirical Observation 4.4).

We also estimated the leading eigenvalue of $D\mathcal{P}|_{f_*}$:

Empirical Observation 4.2 *The eigenvalue of $D\mathcal{P}|_{f_*}$ with the largest modulus is*

$$\lambda \approx -0.017 + 0.040i, \quad |\lambda| \approx 0.044.$$

The small size of λ explains the rapid convergence of the iterates of \mathcal{P} to the fixed point. To obtain this estimate, we write

$$f(z) = z + z^2 + \sum_{k=3}^{\infty} \text{coeff}_k(f)z^k,$$

and consider the spectrum of the $N \times N$ matrix $A = (a_{ij})_{i,j=3\dots N+3}$, with

$$a_{ij} = \frac{\text{coeff}_j(\mathcal{P}(f_* + \varepsilon z^i)) - \text{coeff}_j(f_*)}{\varepsilon},$$

which serves as a finite-dimensional approximation to $D\mathcal{P}|_{f_*}$.

4.2 Computing the Domain of Analyticity of f_*

4.2.1 Computing the Tail of the Domain $\text{Dom}(f_*)$

Computing the tail using an approximate self-similarity near the tip Let us denote

$$t_* \equiv t^{f_*} = \partial\text{Dom}(f_*) \cap \overline{B_0^{f_*}}$$

the endpoint of the tail of the immediate basin of f_* . Let C_R be a repelling fundamental crescent of f_* , and let $w \in C_R$ have the property

$$t_* = \text{ixp} \circ \phi_R(w).$$

Let $k \geq 2$ be such that

$$f_*^k(w) = 0, \text{ so that } f_*^{k-1}(w) = t_*.$$

Denote χ the local branch of $f_*^{-(k-1)}$ which sends t_* to w . Then the composition

$$\nu \equiv \text{ixp} \circ \phi_R \circ \chi$$

is an analytic map defined in a neighborhood of the endpoint t_* , which fixes it:

$$\nu(t_*) = t_*.$$

This point can be found numerically:

Empirical Observation 4.3

$$t_* \approx -779.306 - 643.282i, \text{ and } \nu'(t_*) \approx 0.232 + 0.264i.$$

Thus, we have identified the endpoint of the largest tail of $\text{Dom}(f_*)$. This construction also gives us the means to compute the tail itself. This can be done by successively applying ν to the immediate basin $B_0^{f_*}$, thus pulling it in towards t_* .

Now let $q \in C_R$ be any other preimage of 0:

$$f_*^l(q) = t_* \quad \text{for some } q \in \mathbb{N}.$$

Then $\nu = \text{ixp} \circ \phi_R(q)$ is the endpoint of a different tail in $\partial\text{Dom}(f_*)$. It can be computed by first pulling back the tail of $B_0^{f_*}$ using the inverse branch

$$f_*^{-l} : t_* \mapsto q,$$

and then applying $\text{ixp} \circ \phi_R$.

Computing the tail using the functional equation for an inverse branch A more careful analysis of the tail can be done as follows (Fig. 4.2). Denote by ξ the local branch of f_*^{-1} defined in a slit neighborhood $D_r(0) \setminus [0, r)$ for some small value of r , that sends $0 \mapsto t_*$. We can write the renormalization fixed point equation for this particular branch:

$$\xi = \psi_R \circ \xi \circ \psi_A^{-1}, \tag{4.1}$$

where $\psi_R = \chi \circ \text{ixp} \circ \phi_R$, and ψ_A^{-1} is the appropriately chosen branch of $(\text{ixp} \circ \phi_A)^{-1}$ (thus the “self-similarity” of the tail is exponential, rather than linear). We are going to use the renormalization equation (4.1) *inductively* to compute $\xi(z)$ for sufficiently small values of z , and thus plot the tail.

Representing the numbers in the image of the tail Numerical computations indicate that the value of $r = 0.0002$ is sufficiently small for our needs, and for $|z| < r$ the difference between the left and the right sides of (4.1) is of the order of 10^{-11} . The values of z for which we would like to evaluate $\xi(z)$ become too small to be represented by the standard double precision numbers (and even too small for their logarithms to be so represented). We write

$$s(t) = \exp(2\pi t),$$

and choose \hat{t} so that

$$\exp(-2\pi\hat{t}) = 0.0002, \quad \text{that is } \hat{t} = 1.3555\dots$$

We then represent a small positive number x as

$$x = \frac{1}{s^k(t)},$$

for the unique choices of $t \in [\hat{t}, s(\hat{t}))$, and an iterate $k \in \mathbb{N}$.

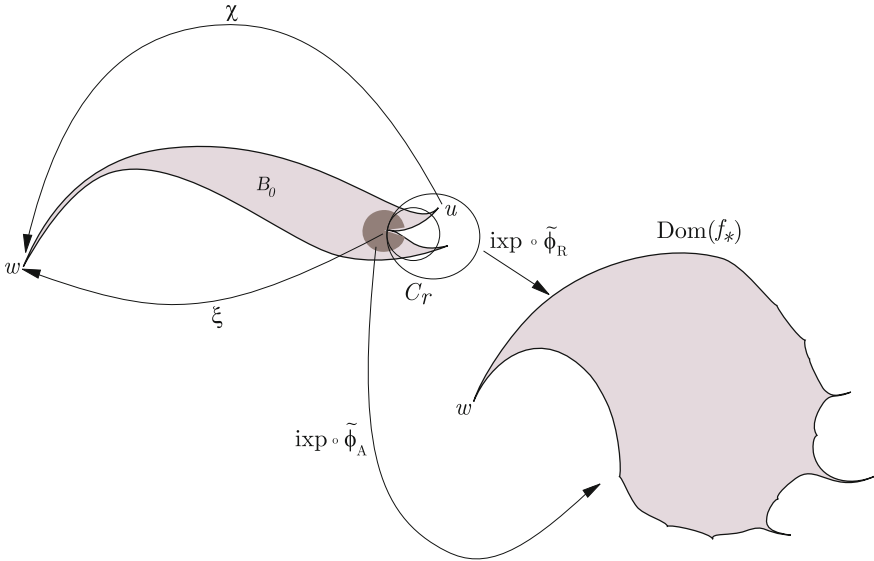


Fig. 4.2 The inverse branches used in computing the tail of $\text{Dom}(f_*)$

We can write any complex number z with $|z| < r$ uniquely as

$$z = (k, t, \theta) \equiv \frac{\exp(2\pi i \theta)}{s^k(t)}, \quad 0 \leq \theta < 1.$$

Note that this representation of small numbers makes it very easy to compute logarithms. In particular,

$$\text{ixp}^{-1}((k, t, \theta)) = \theta + is^{k-1}(t).$$

The next step in applying (4.1) is to apply ϕ_A^{-1} to the right-hand side of the equation. From the first two terms in the asymptotics of

$$\phi_A(z) = -\frac{1}{z} + O(\log |z|) \quad \text{for small } z,$$

it follows that

$$\phi_A^{-1}(y) = -\frac{1}{y + O(\log |y|)} \quad \text{for large } |y|.$$

A numerical estimate shows that for $|y| \geq 10^{18}$, the $O(\log |y|)$ term disappears into the round-off error when added to y . Thus

$$\psi_A^{-1}((k, t, \theta)) \approx -\frac{1}{\theta + is^{k-1}(t)} \approx is^{k-1}(t) = (k - 1, t, 1/4),$$

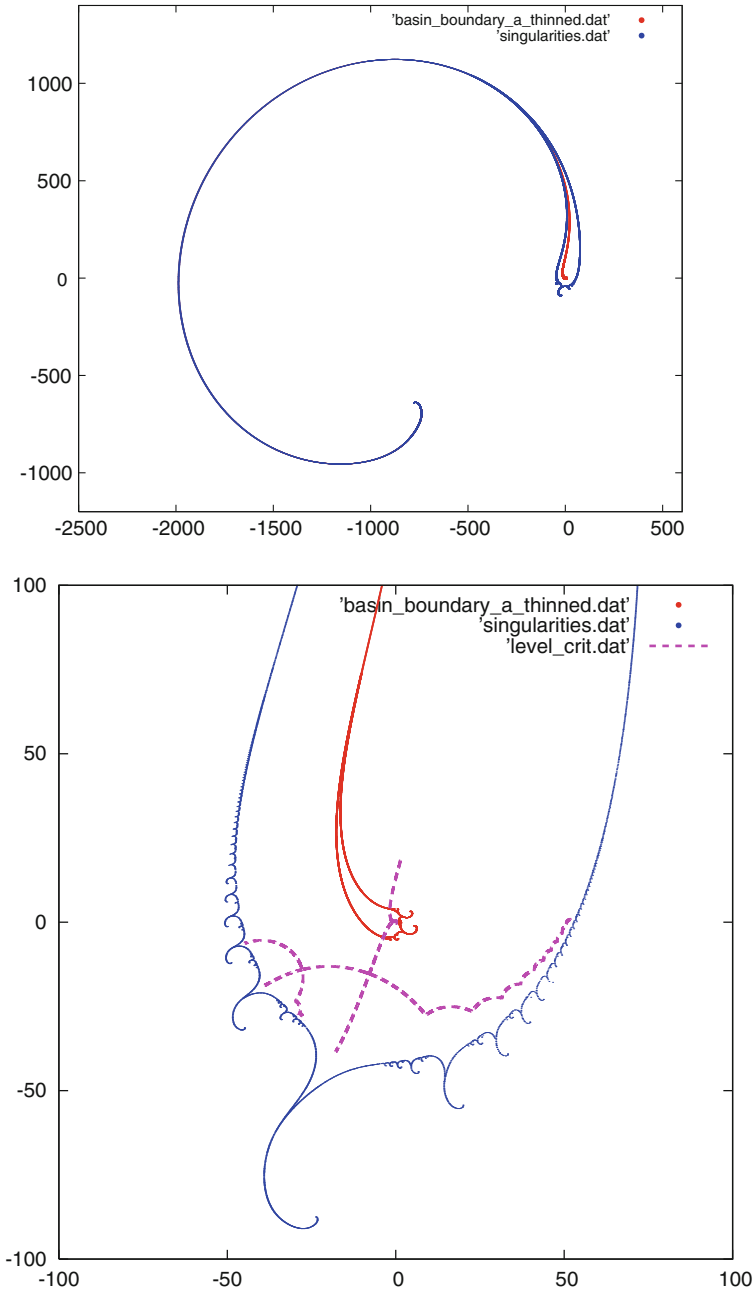


Fig. 4.3 The domain of analyticity of f_* and the boundary of the immediate parabolic basin $B_0^{f_*}$. In the second figure, a part of the critical level curve of f_* is also indicated

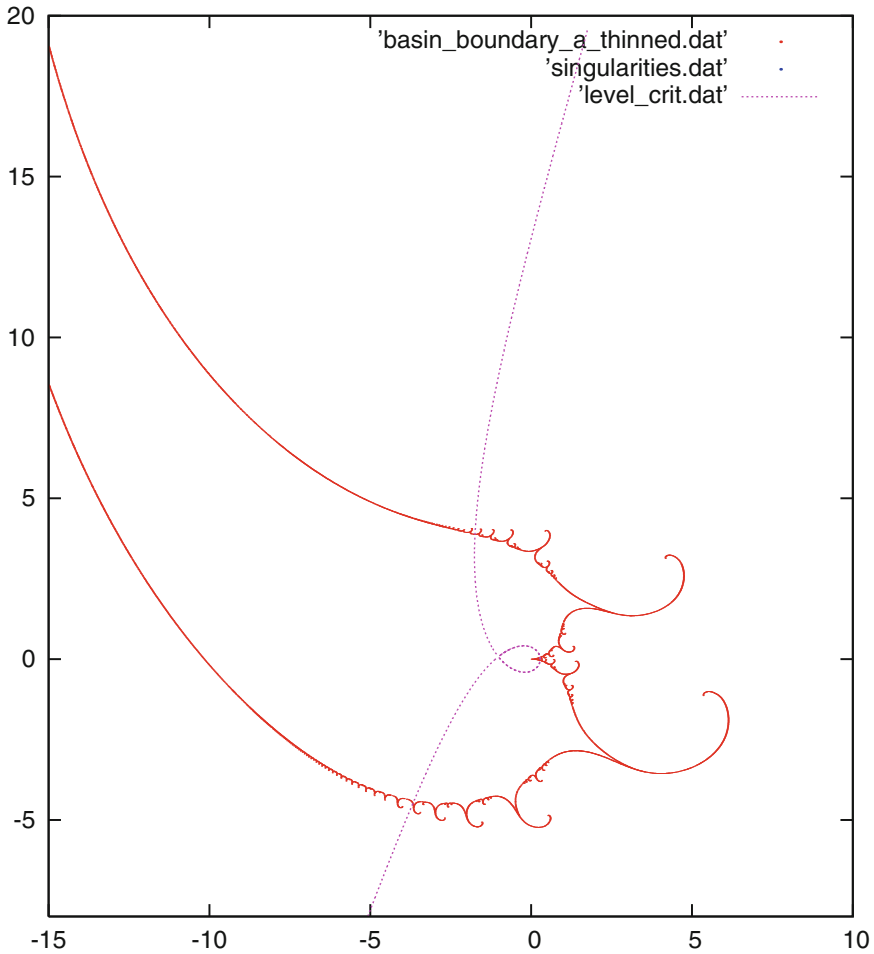


Fig. 4.4 A blow-up of the boundary of the immediate basin of f_* in the vicinity of the parabolic point

provided $s^{k-1}(t) \geq 10^{18}$. A direct estimate shows that for either $k \geq 3$, or $k = 2$ and $t > 18 \log 10/2\pi \approx 6.596$, the last inequality will hold.

The size of the domain of analyticity To draw the pictures of the domain of analyticity of the fixed point of f_* (Figs. 4.3 and 4.4) we employed the following strategy. First, a periodic orbit of period 2 in ∂B_0 was identified. Its preimages give a rough outline of ∂B_0 , but become sparse near the “tails”, which are not visible in this initial outline. At the next step, the large “tail” of B_0 is computed as described above. Finally, its preimages are used to fill in the remaining gaps in ∂B_0 .

As the final step, we calculate the boundary of $\text{Dom}(f_*)$ as

$$\partial \text{Dom}(f_*) = \text{ixp} \circ \phi_R(\partial B_0 \cap P_R).$$

An empirical estimate of the inner radius of $\text{Dom}(f_*)$ around the origin allows us to formulate the following observation (see Fig. 4.3):

Empirical Observation 4.4 *The radius of convergence of the Taylor expansion of f_* at the origin is $R \approx 41$.*